Journal of Peptide Science
J. Pept. Sci. 2007; **13**: 269–279
Published online in Wiley InterScience (www.interscience.wiley.com). DOI: 10.1002/psc.846

JOURNAL OF PEPTIDE SCIENCE

The solution structure of horseshoe crab antimicrobial peptide tachystatin B with an inhibitory cystine-knot motif

NAOKI FUJITANI,[a] TAKAHIDE KOUNO,[b] TAKU NAKAHARA,[a] KENJI TAKAYA,[a] TSUKASA OSAKI,[c‡] SHUN-ICHIRO KAWABATA,[c] MINEYUKI MIZUGUCHI,[b] TOMOYASU AIZAWA,[d] MAKOTO DEMURA,[a] SHIN-ICHIRO NISHIMURA[a,e*] and KEIICHI KAWANO[d*]

[a] Division of Advanced Chemical Biology, Graduate School of Advanced Life Science, Frontier Research Center for Post-Genome Science and Technology, Hokkaido University, Sapporo 001-0021, Japan
[b] Faculty of Pharmaceutical Sciences, University of Toyama, Toyama 930-0194, Japan
[c] Department of Biology, Faculty of Sciences, Kyushu University, Fukuoka 812-8581, Japan
[d] Division of Biological Sciences, Graduate School of Science, Hokkaido University, Sapporo 060-0810, Japan
[e] Drug-Seeds Discovery Research Laboratory, National Institute of Advanced Industrial Science and Technology (AIST), Sapporo 062-8517, Japan

Received 22 November 2006; Revised 15 January 2007; Accepted 24 January 2007

Abstract: Tachystatin B is an antimicrobial and a chitin-binding peptide isolated from the Japanese horseshoe crab (*Tachypleus tridentatus*) consisting of two isopeptides called tachystatin B1 and B2. We have determined their solution structures using NMR experiments and distance geometry calculations. The 20 best converged structures of tachystatin B1 and B2 exhibited root mean square deviations of 0.46 and 0.49 Å, respectively, for the backbone atoms in Cys^4-Arg^{40}. Both structures have identical conformations, and they contain a short antiparallel β-sheet with an inhibitory cystine-knot (ICK) motif that is distributed widely in the antagonists for voltage-gated ion channels, although tachystatin B does not have neurotoxic activity. The structural homology search provided several peptides with structures similar to that of tachystatin B. However, most of them have the advanced functions such as insecticidal activity, suggesting that tachystatin B may be a kind of ancestor of antimicrobial peptide in the molecular evolutionary history. Tachystatin B also displays a significant structural similarity to tachystatin A, which is member of the tachystatin family. The structural comparison of both tachystatins indicated that Tyr^{14} and Arg^{17} in the long loop between the first and second strands might be the essential residues for binding to chitin. Copyright © 2007 European Peptide Society and John Wiley & Sons, Ltd.

Keywords: tachystatin B; antimicrobial peptide; inhibitory cystine-knot (ICK) motif; innate immunity; NMR; structure determination

INTRODUCTION

Innate immunity develops earlier than acquired immunity and is identified in all multicellular organisms as an essential system for host defense against bacterial, fungal, and viral pathogens [1–3]. Therefore, the innate immune system is an important object of study with regard to biological and immunological host defense reactions. Unlike vertebrate animals, invertebrate animals and plants have no acquired immune system. Because of the lack of acquired immunity, invertebrate animals and plants have developed unique mechanisms to recognize invading pathogens. Antimicrobial peptides are the principals of innate immunity. To date, many antimicrobial peptides have been found and subjected to structural analyses. On the basis of their structure, they are mostly classified into three categories: (i) linear or α-helical peptides without disulfides, (ii) peptides with a high content of one or two types of amino acids, and (iii) cysteine-rich peptides [4,5]. Some structures have been proposed for drug design because of their high stability to heat and protease digestion [6,7].

The horseshoe crab is well known as a 'living fossil' with its lineage of greater than two hundred million years, suggesting that the horseshoe crab has an excellent innate immune system. To date, more than 47 defense molecules have been identified in the hemocytes and the hemolymph plasma of the Japanese horseshoe crab (*Tachypleus tridentatus*) [8–10]. The hemolymph plasma of *T. tridentatus* contains granular hemocytes, which are highly sensitive to lipopolysaccharides [11,12]. After the stimulation of lipopolysaccharides, the defense molecules in the granular hemocytes are immediately secreted by exocytosis. These hemocytes consist of two types of granules, called *large* and *small* granules. The large granule selectively stores defense molecules including coagulation factors, protease inhibitors, and lectins, and the small one preserves at least six types of peptides categorized into antimicrobial substances [8–13]. From a structural point of view, several three-dimensional structures

*Correspondence to: Shin-Ichiro Nishimura, Division of Advanced Chemical Biology, Graduate School of Advanced Life Science, Frontier Research Center for Post-Genome Science and Technology, Hokkaido University, Sapporo 001-0021, Japan;
e-mail: shin@glyco.sci.hokudai.ac.jp
Keiichi Kawano, Division of Biological Sciences, Graduate School of Science, Hokkaido University, Sapporo 060-0810, Japan;
e-mail: kawano@sci.hokudai.ac.jp
‡Present address: National Cardiovascular Center Research Institute, Suita, Osaka 565–8565, Japan.

of defense molecules in *T. tridentatus*, tachylectin-1 (unpublished), -2 [14], -5A [15], coagulogen [16], tachyplesin I [17,18], tachycitin [19], and tachystatin A [20], have been determined to date, and have lead to the understanding of the host defense mechanism of the horseshoe crab.

Among the antimicrobial molecules of *T. tridentatus*, the tachystatin family in the small granule of the hemocyte is one of the most potent molecules exhibiting a strong and wide spectrum of antimicrobial activity against fungi and Gram-negative and -positive bacteria [21]. Furthermore, tachystatins have chitin-binding activity as a common property, with the antimicrobial peptide stored in the small granule of horseshoe crab hemocytes [21]. As chitin is a major component of the fungus cell wall, this activity might be important for the recognition of fungi by the antimicrobial peptide. The tachystatin family consists of three types of peptides, tachystatin A, B, and C (Figure 1), which are highly cationic peptides stabilized by three disulfide bonds. They have the preserved cysteine residues on primary structures with neurotoxins isolated from spider venom (Figure 1) [21]. The horseshoe crab is a close relative of spiders in evolutionary history and, therefore, tachystatins and spider toxins may have evolved from the common ancestor of ancient arthropods.

Here we show the structural analyses of tachystatin B using NMR experiments. Tachystatin B consists of two isopeptides with 42 amino acid residues; tachystatin B1 contains Val and Ser residues at the second and third positions, respectively, and tachystatin B2 contains Ile and Thr residues at these corresponding sites (Figure 1). Tachystatin B1 and B2 (Tachystatin B) exhibit significantly strong antimicrobial activity against fungi (*C. albicans* and *P. pastoris*) and Gram-positive bacteria (*S. aureus*). However, unlike tachystatin A and C, they are inactive against Gram-negative bacteria (*Escherichia. coli*) [21]. In this study, we determine the conformation of tachystatin B in order to better understand the different activity of tachystatins, and also to extend our understanding of the molecular evolution and the structure–activity relationships of the tachystatin family.

MATERIALS AND METHODS

Sample Preparation for NMR

Hemocyte debris from the Japanese horseshoe crab (*Tachypleus tridentatus*) was prepared according to the methods of Nakamura *et al.* [22], and tachystatin B was also purified as described previously [21]. Tachystatin B consists of isopeptides, tachystatin B1, and tachystatin B2. The abundance ratio of tachystatin B1 and tachystatin B2 is 3 : 2 [21]. The NMR samples for the structure determination of tachystatin B were prepared by dissolving the lyophilized peptide in aqueous solvents ($H_2O : D_2O = 9 : 1$ or 99.8% D_2O). The concentration of the sample was 0.73 mM, which was determined by the calculated molar extinction coefficient of 7265 M^{-1} cm^{-1} of tachystatin B at 280 nm UV absorption. The unbuffered pH was adjusted to 3.5 by DCl and NaOD, conditions identical to the NMR analyses of tachystatin A [20].

NMR Spectroscopy

NMR spectra were collected at 25 and 37 °C with Bruker Avance 600 and 800 spectrometers at 600.13 and 800.23 MHz for proton frequency, respectively, equipped with Cryo-probe.

For the determination of the solution structure of tachystatin B, spectra were recorded using two-dimensional homonuclear double quantum filtered correlation spectroscopy (DQF-COSY) [23], total correlation spectroscopy (TOCSY) with MLEV-17 sequence [24,25], and nuclear Overhauser effect spectroscopy (NOESY) [26] in the indirect dimension using States-TPPI phase cycling. TOCSY experiments were applied for a spin-locking time of 60 ms, and NOESY experiments were carried out with mixing times of 100, 200, and 400 ms. The suppression of the water signal was achieved by presaturation during the relaxation delay (1 s) and by a 3–9–19 WATERGATE pulse sequence with field gradient [27,28]. TOCSY and NOESY spectra were acquired with 2048 × 512 frequency data points and were zero-filled to yield 2048 × 2048 data matrices. DQF-COSY with 8192 × 512 frequency data points was also recorded and zero-filled to yield an 8192 × 8192 matrix in order to measure the coupling constants. The sweep widths of 6009.62 and 14 367.82 Hz were applied in 600 and 800 MHz

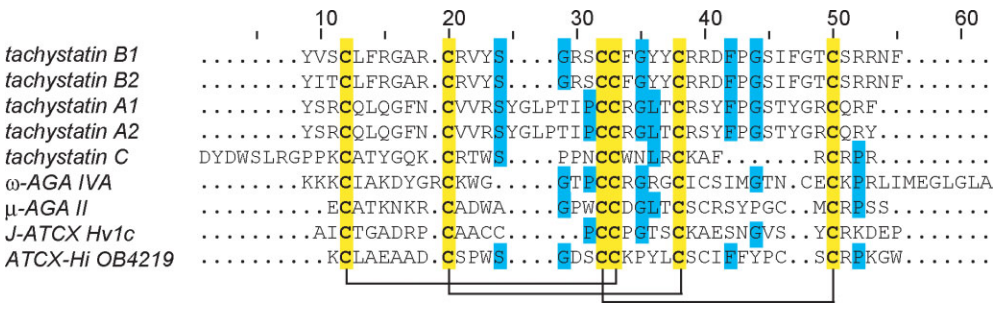

Figure 1 Alignment of the amino acid sequence of the tachystatin family and atracotoxins. The conserved cysteine residues are indicated by yellow boxes, and the other consensus residues with tachystatins are indicated by blue boxes. Three pairs of disulfide bonds are represented by lines. The representative neurotoxic peptides isolated from spider venom also preserve the disulfide pattern.

DOI: 10.1002/psc

NMR, respectively. Time domain data in both dimensions were multiplied by a sine bell window function with a 90° phase shift prior to Fourier transformation. All NMR data were processed by the NMRPipe software [29], and analyzed using the XEASY program [30]. Sequence-specific resonance assignments were achieved according to the standard methods for small proteins established by Wüthrich and coworkers [31]. Stereospecific assignments for methylene protons were carried out by analyzing the intensities of intraresidue NOE between the amide and beta protons and coupling constants observed in the exclusive correlation spectroscopy (E-COSY) spectrum [32]. In order to determine the amide protons with a slow exchange rate, TOCSY spectra were acquired 24 h after dissolving the lyophilized peptide in D_2O.

For the NMR diffusion experiment to determine the diffusion coefficient d and estimate the effective hydrodynamic radius R_H of tachystatin B, 2.5 µl of a 1% solution of dioxane in D_2O was added to the NMR sample in D_2O as an internal reference (final concentration of dioxane was approximately 0.0008% (v/v)) [33,34]. Diffusion-ordered spectroscopy (DOSY) [35] spectra were recorded by 32 scans at each step with the gradient strength increasing in 25 steps from 1.25 to 60% of the maximum gradient strength. The gradient pulse length δ was set to 4 ms, and an echo time Δ of 100 ms was applied. The diffusion coefficient d was determined by the analysis of DOSY spectrum, and R_H was calculated by the following equation [33]:

$$R_H^{prot} = (d_{dioxane}/d_{prot}) \times R_H^{dioxane} \quad (1)$$

where R_H^{prot} and $R_H^{dioxane}$ are the effective hydrodynamic radii of the protein and the dioxane reference, respectively, and d_{prot} and $d_{dioxane}$ are the measured diffusion coefficients of the protein and the dioxane, respectively. $R_H^{dioxane}$ was taken as 2.12 Å [34]. NMR diffusion data were processed using the mode for analyzing the relaxation time in the Bruker Xwinnmr 3.1 program. Moreover, the theoretical hydrodynamic radius was calculated using the following equation [34]:

$$R_H = (4.75 \pm 1.11) \times N^{0.29\pm0.02} \quad (2)$$

where N is the number of residue in the protein.

Structure Calculation

Three-dimensional structures of tachystatin B were calculated using the CNS 1.1 program [36] with standard protocols for distance geometry-simulated annealing and refinement. A total of 377 distance restraints and 55 dihedral angle ϕ restraints were used to calculate the family of the structure. Distance restraints for the calculations were estimated from the cross-peak intensities in NOESY spectra with a mixing time of 100 ms; the estimated restraints were then classified into four categories (strong, medium, weak, and very weak) and were assigned upper limits of 2.8, 3.5, 5.0, and 6.0 Å, respectively.

In the first stage of structure determination, the monomeric structures of tachystatin B were calculated using only the interproton distance information. After the validation of fulfilling distance restraints for the obtained structure, the restraints of the dihedral angle ϕ were adopted for structure calculation. When the coupling constant $^3J_{HN\alpha}$ was more than 8.0 Hz and less than 6.0 Hz, the dihedral angle ϕ was constrained to $-120 \pm 30°$ and $-60 \pm 30°$, respectively [31]. Additionally, a broad dihedral angle constraint was used to constrain the ϕ angle between $-35°$ and $-180°$ for the residues in which the coupling constant could not be reliably determined [37]. In the final step of structure determination, hydrogen-bond constraints were used as distance constraints of 1.5–2.5 Å between amide protons and carbonyl oxygen, and 2.5–3.5 Å between amide nitrogen and amide protons.

All analyses of the root mean square deviation (RMSD) values and the solution structures of tachystatin B were performed with the PROCHECK [38] and MOLMOL [39] programs.

RESULTS AND DISCUSSION

NMR Analyses for the Structure Determination of Tachystatin B

Preceding the structure determination, a DOSY measurement with the stimulated echo sequence [35] was carried out to determine whether tachystatin B is a monomer or an oligomer. In the DOSY spectra (Figure 2(a)), the signals derived from tachystatin B1 and B2 were completely overlapped, meaning that both isomers had identical diffusion coefficients d. Its value was found to be 1.338×10^{-10} m^2 s^{-1}, resulting in the effective hydrodynamic radius R_H of tachystatin B of 13.27 Å by Eqn (1). The theoretical R_H value was found to be 14.04 Å by Eqn (2). If tachystatin B constructs a dimer (84 residues), the R_H will be 16.22 Å by Eqn (2). Therefore, tachystatin B exists as a monomeric conformer in the NMR sample condition.

All acquired NMR spectra for the structure determination showed good signal dispersion at 27 and 37 °C (Figure 2(b)), enabling the complete assignments by a usual series of two-dimensional NMR spectra, and the chemical shift data have been deposited into the databank BioMagResBank (http://www.bmrb.wisc.edu/) with the accession numbers 7171 and 7173 for tachystatin B1 and B2, respectively. In the N-terminal region, the residues of Val^2-Ser^3 for tachystatin B1 and Ile^2-Thr^3 for tachystatin B2 could be observed separately with weak intensity. The NMR spectra of tachystatin B clearly showed one set of signals for the residues consisting of Cys^4-Phe^{42} without fatal overlap, suggesting that tachystatin B1 and B2 had identical conformations in the region of Cys^4-Phe^{42}.

NOESY experiments revealed that the sequential connectivities between H^α and NH ($d_{\alpha N}$) were observed with strong intensity over the length of tachystatin B; on the other hand, the sequential connectivities between amide protons (d_{NN}) were observed exiguously. Furthermore, 14 residues were found to have a coupling constant between those of the H^α and NH proton ($^3J_{HN\alpha}$) of more than 8.0 Hz. These NOE and coupling constant information suggested that tachystatin B might be rich in β- or extended structures without the helical

DOI: 10.1002/psc

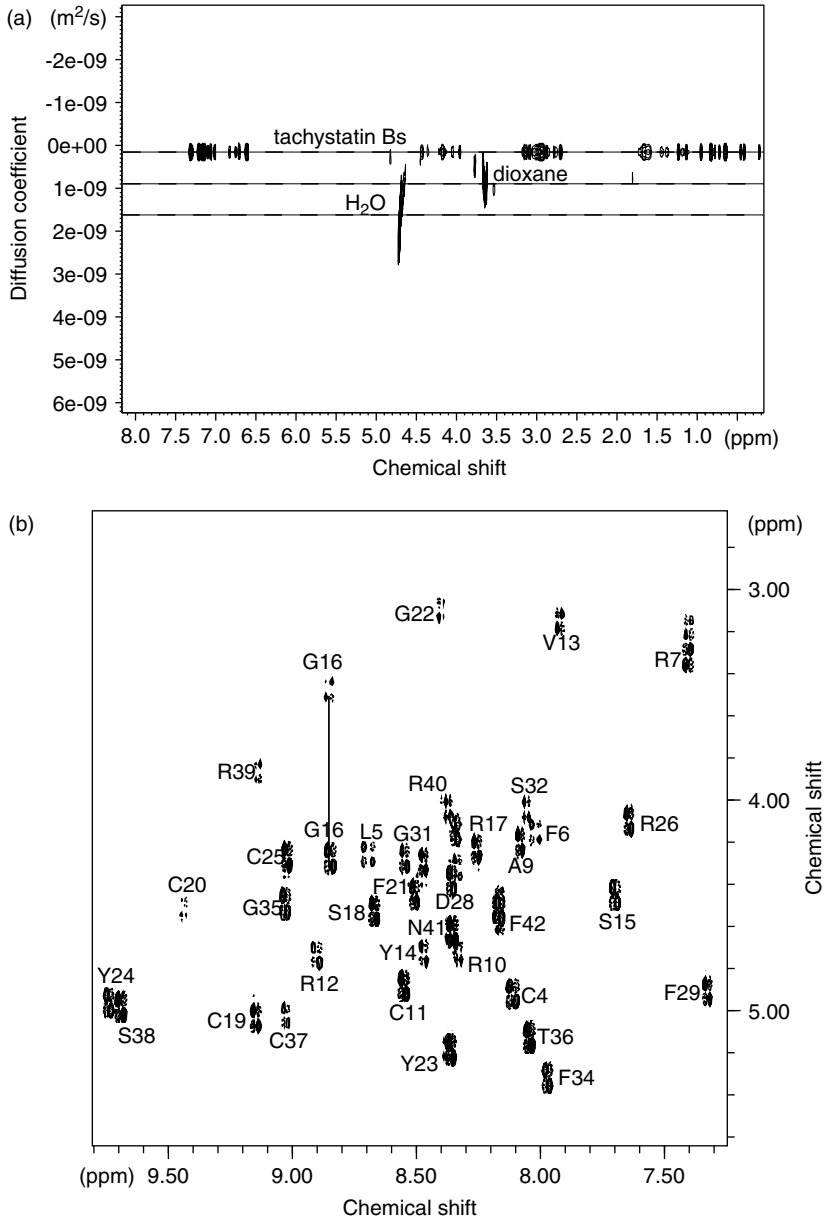

Figure 2 NMR spectra of tachystatin B. (a) DOSY spectrum of tachystatin B with internal reference of dioxane. The signals derived from tachystatin B1 and B2 were completely overlapped, suggesting that they have identical diffusion constants. (b) Fingerprint region of DQF-COSY of tachystatin B. The assignments are labeled on the region of residues 4–42. The residues 2 and 3 were observed with weak intensities. Both spectra were recorded at 27 °C.

conformation. The sequential NOEs and the coupling constant information are summarized in Figure 3(a).

The hydrogen–deuterium exchange using the TOCSY measurement, which was recorded 24 h after dissolving the sample in D_2O, revealed that eight residues, Cys^{11}, Tyr^{23}, Tyr^{24}, Arg^{26}, Gly^{35}, Thr^{36}, Cys^{37}, and Ser^{38}, had slow exchange rates (Figure 3(a)). This suggested that these residues form hydrogen bonds to construct the stable conformation. Analyzing the NOE network, coupling constants, and hydrogen-bond information suggested that tachystatin B contains a triple-stranded antiparallel β-sheet with $+2x$, -1 topology and a tight turn as shown in Figure 3(b).

Solution Structure of Tachystatin B

The solution structures of tachystatin B were calculated on the CNS 1.1 software with 377 distance restraints, 55 dihedral angle (ϕ and χ_1) constraints, and 8 pairs of hydrogen bonds, from which 20 structures with low potential energy could be selected, and the coordinates and the restraint data for tachystatin B1 and B2 have been deposited into the Protein Data Bank with accession codes 2DCV and 2DCW, respectively. Structural statistics and the determined structures are represented in Table 1 and Figure 4, respectively. Because identical NOEs were observed

DOI: 10.1002/psc

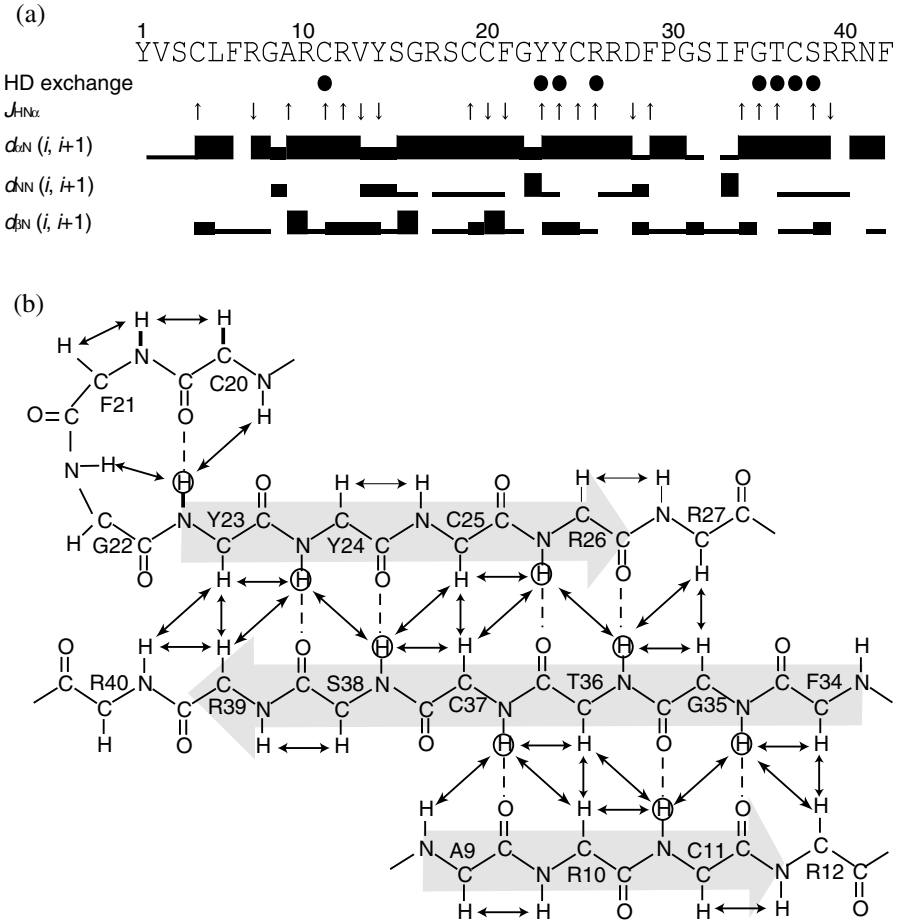

Figure 3 Summary of NMR assignments and the secondary structures observed in tachystatin B. (a) The amide proton, still visible in TOCSY spectrum 24 h after exchange into D_2O, is represented by filled circles. The coupling constants $^3J_{HN\alpha}$ more than 8.0 Hz and less than 6.0 Hz are indicated by upward and downward arrows, respectively. The sequential NOEs, $d_{\alpha N}$, d_{NN}, and $d_{\beta N}$, are represented by bars, and the bar thickness corresponds to the NOE intensity. (b) The schematic diagram of a β-sheet and a β-turn. The observed NOEs are shown by arrows. The encircled protons represent the slowly exchanging amides, and the hydrogen bonds are indicated by dotted lines.

for tachystatin B1 and B2, same constraints were used for the region of Cys[4]-Phe[42] of both peptides, resulting in identical conformations for both peptides (Figure 4(a)), and there was no statistically meaningful difference between the two peptides in the structural statistics (Table 1). The RMSD for the backbone and for the heavy atoms of the ordered region (Cys[4]-Arg[40]) of tachystatin B1 were found to be 0.46 ± 0.08 Å and 1.57 ± 0.17 Å, respectively, and those of tachystatin B2 were found to be 0.49 ± 0.10 Å and 1.52 ± 0.18 Å, respectively, when the corresponding regions were superimposed. The obtained structures showed that tachystatin B had well-converged structures on the whole molecule, though the initial three residues of the *N*-terminal and the final two residues of the *C*-terminal regions represented disordered structures due to the insufficiency of long- and medium-range NOE.

The obtained structures of tachystatin B demonstrated a triple-stranded antiparallel β-sheet with a topology of $+2x$, -1(Figure 4(b)), corresponding to the NMR analyses shown in Figure 3(b). The first (β1), second (β2), and third (β3) strands were constructed by residues Ala[9]-Arg[12], Tyr[23]-Arg[26], and Gly[35]-Arg[39], respectively. A tight turn formed by Cys[20]-Tyr[23] was also identified as a β-turn with an intraturn hydrogen bond between the carbonyl oxygen of Cys[20] and the amide proton of Tyr[23]. On the basis of the structural analyses of the 40 lowest energy conformers of tachystatin B (20 structures of tachystatin B1 and 20 structures of tachystatin B2), the average dihedral angles ϕ and ψ of Phe[21], the second position of the β-turn, were found to be $-63.0 \pm 4.0^\circ$ and $118.3 \pm 5.8^\circ$, respectively, and those of Gly[22], the third position of the β-turn, were found to be $92.9 \pm 9.5^\circ$ and $5.2 \pm 15.3^\circ$, respectively, suggesting that this was categorized into a type II β-turn. Furthermore, the region including Phe[6]-Ala[9] also formed a tight turn similar to the type II β-turn in the light of dihedral angles. The average dihedral angles ϕ and ψ of Arg[7] were found to be $-56.4 \pm 3.0^\circ$ and $136.0 \pm 6.1^\circ$, respectively, and those of Gly[8] were

DOI: 10.1002/psc

Table 1 Structural statistics for 20 structures of tachystatin B calculated by CNS1.1 [36]

	Tachystatin B1	Tachystatin B2
Average potential energies (kcal mol^{-1})		
$E_{overall}$	21.00 ± 0.93	21.00 ± 0.88
E_{bond}	0.40 ± 0.08	0.40 ± 0.07
E_{angle}	15.60 ± 0.31	15.72 ± 0.29
E_{impr} (energy of improper torsion angles)	0.60 ± 0.05	0.64 ± 0.06
E_{VDW} (van der Waals repulsion energy)	3.65 ± 0.56	3.66 ± 0.58
E_{NOE} (square-well NOE potential energy)	0.63 ± 0.24	0.73 ± 0.34
E_{cdih} (dihedral potential energy)	0.12 ± 0.03	0.13 ± 0.03
Deviation from idealized geometry		
Bonds (Å)	0.0008 ± 0.00008	0.0008 ± 0.00007
Angles (°)	0.2931 ± 0.0028	0.2929 ± 0.0028
Impropers (°)	0.0992 ± 0.0043	0.1023 ± 0.0047
Pairwise RMSD for residues Cys^4-Arg^{40} (Å)		
Backbone atoms (N, C$^\alpha$, C′)	0.46 ± 0.08	0.49 ± 0.10
All heavy atoms	1.57 ± 0.17	1.52 ± 0.18
Ramachandran plot (%)		
Most favored regions	77.5	74.0
Additional allowed regions	22.4	25.7
Generously allowed regions	0.1	0.3
Disallowed regions	0.0	0.0
Number of experimental restraints		
Intraresidue ($\|i-j\|=0$)	87	87
Sequential ($\|i-j\|=0$)	135	135
Medium range ($2 \le \|i-j\| \le 4$)	58	58
Long range ($\|i-j\| \ge 0$)	97	97
Dihedral angles (ϕ, χ_1)	55	55
Hydrogen bonds	8	8

found to be $86.8 \pm 9.5°$ and $21.8 \pm 14.5°$, respectively. However, there was no capacity to form an intraturn hydrogen bond and, therefore, this turn consisting of Phe^6-Ala^9 was defined as a miscellaneous type β-turn.

Along with the stable secondary structures, three pairs of disulfides greatly contribute to stabilize the solution structure of tachystatin B. The first bridge, Cys^4-Cys^{20}, connects the *N*-terminal loop and β-turn consisting of Cys^{20}-Tyr^{23}; the second bridge, Cys^{11}-Cys^{25}, is the interstrand bridge crosslinking strands β1 and β2; and the third bridge, Cys^{19}-Cys^{37}, is extended from strand β3 to the loop linking β1 and β2. These disulfide bonds construct a typical inhibitor cystine knot (ICK) motif (Figure 4(c),) [40,41], in which the disulfide bond Cys^{19}-Cys^{37} penetrate through a closed ring formed by two disulfides (Cys^4-Cys^{20} and Cys^{11}-Cys^{25}) and two segments of the backbone (Cys^4-Cys^{11} and Cys^{20}-Cys^{25}). A typical ICK motif incorporates a triple-stranded antiparallel β-sheet stabilized by a cystine knot [40,41]. In general, this fold satisfies the following amino acid consensus, $CX_{3-7}CX_{3-6}CX_{0-5}CX_{1-4}CX_{4-13}C$, where X can be any amino acid and subscript numbers represent the number of the residue X [41]. This motif has widely been found in various peptides from phylogenetically different sources including cone snails, spiders, plants, and fungi, and it has been reported that most peptides with this motif are defined as antagonists to voltage-gated ion channels or insecticidal neurotoxins [40,41]. The structural features of tachystatin B satisfy the conditions necessary for an ICK motif, although they have one too many residue of the consensus sequence between the second and the third cystine.

Tachystatin B is a highly cationic peptide with a calculated isoelectric point of 12.0 [42], as a result of the high proportions of arginine (eight residues), though only one negatively charged residue (Asp^{28}) could be found in the peptide. The electrostatic potential represented in Figure 5 shows that the positively charged area is widely distributed on the surface of tachystatin B. In addition, tachystatin B was also rich in hydrophobic residues. It has been reported that a hydrophobic core in peptides with an ICK motif could be constructed by two *C*-terminal disulfide bridges and a hydrophobic residue protruding from the *N*-terminal loop or the segment between the fourth and fifth cystines [43]. Actually, the obtained structure of tachystatin B also indicated that two disulfides, Cys^{11}-Cys^{25} and Cys^{19}-Cys^{37} (indicated by red in Figure 4(d)), were located in the core of the molecule producing a hydrophobic environment and, furthermore, the side chain of Ile^5 in the *N*-terminal

DOI: 10.1002/psc

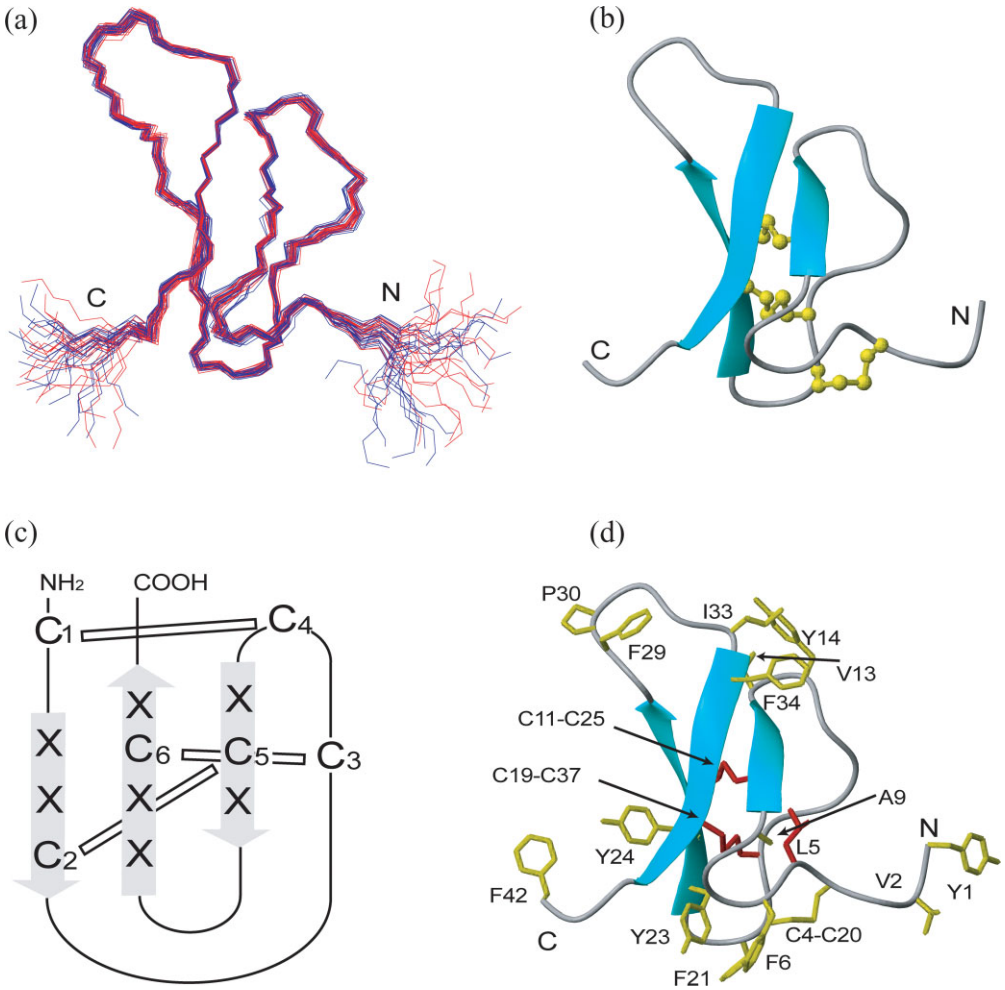

Figure 4 The solution structure of tachystatin B with an inhibitory cystine-knot (ICK) motif. Tachystatin B has a triple-stranded antiparallel β-sheet stabilized by three pairs of disulfides with the ICK motif. (a) The 20 converged structures of tachystatin B1 (red; PDB ID: 2DCV) and B2 (blue; PDB ID: 2DCW) superimposed by the backbone atoms of residues Cys^{4}-Arg^{40}, showing that tachystatin B1 and B2 have identical conformations. (b) The ribbon model of the lowest energy structure of tachystatin B1. Three pairs of disulfide bonds are represented by ball-sticks. (c) Consensus structure for the ICK motif proposed by Pallaghy *et al.* [40,41]. The β-strands are shown by gray arrows and the disulfide bonds are represented by bars. The consensus residues are shown as one-letter symbol C (cystine) and X (not necessarily cystine residue). (d) The same model as in (B) with the side chain heavy atoms (stick) of all the hydrophobic residues. The characteristic residues for the construction of hydrophobic core in the ICK motif are colored red.

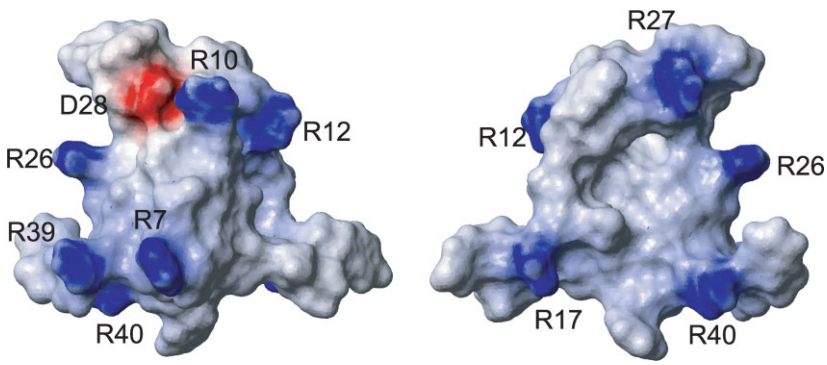

Figure 5 Electrostatic surface potential of tachystatin B1. The positively and negatively charged regions are colored blue and red, respectively. All charged residues in tachystatin B1 are labeled. The structure drawn on the left is in the same orientation as Figure 4 and the structure on the right is rotated 180° with respect to that on the left.

DOI: 10.1002/psc

loop trended inside the molecule and contributed to the formation of a hydrophobic core with disulfide bonds. This hydrophobic patch was supported by the results of NOESY experiments, which showed several long-range NOEs between Ile[5] and Ala[9], Cys[11], Cys[19] and Cys[20]. Additionally, the other hydrophobic residues were clustered in the regions including a type II β-turn from Cys[20] to Tyr[23], and an interloop hydrophobic patch constructed by Val[13], Tyr[14], Ile[33], and Phe[34] was also found in the determined structure (Figure 4(d)). Both regions were located on the surface of the molecule. Generally, it is suggested that antimicrobial activity is exerted by a hydrophobic core and cationic residues exposed on the molecular surface [44]. Tachystatin B has both hydrophobic and hydrophilic regions produced by a cystine-knot motif and enrichment of arginine residues, which play an important role in antimicrobial activity.

Structural Comparisons of Tachystatins with the ICK Peptides

We had previously determined the solution structure of tachystatin A, which is a constituent of the tachystatin family [21]. Tachystatin A is also the isopeptide consisting of tachystatin A1 and A2 with 42% sequential homology to tachystatin B (Figure 1) [20]. In order to investigate the structure–function relationship, both solution structures were compared, which showed that tachystatin A and B showed striking similarity (Figure 6(a)). Both peptides have an ICK motif. The locations of the β-turns were also identical in both molecules. The RMSD of the backbone atoms of the core ICK motif including three β-strands and two β-turns was found to be 1.00 Å when the corresponding regions were fitted (backbone atoms Cys[4]-Cys[11], Cys[19]-Arg[26], and Phe[34]-Arg[39] of tachystatin B1 fitted to the backbone atoms Cys[4]-Cys[11], Cys[23]-Arg[30], and Tyr[38]-Arg[43] of tachystatin A2, respectively). Interestingly, in spite of the significant structural similarity between tachystatin A and B, they differ greatly in the antimicrobial activity against *E. coli*. Tachystatin A exerts activity against *E. coli* (25 μg/ml of 50% growth inhibitory concentration, IC_{50}); on the other hand, even 100 μg/ml of tachystatin B does not exhibit any activity against *E. coli* [21]. It has been reported that differences in overall folding and activity of peptides with ICK motifs may be determined by the number of residues in the loops, as well as differences in the primary sequence [45]. Indeed, the major structural difference between tachystatin A and B is the long loop between strands β1 and β2. This loop of tachystatin B is shorter than that of tachystatin A and includes a positively charged residue Arg[17], whereas that of tachystatin A is rich in hydrophobic residues without a charged residue. Tachystatin A exerts the antimicrobial activity in a manner similar to the defensin family using a distinct amphiphilic

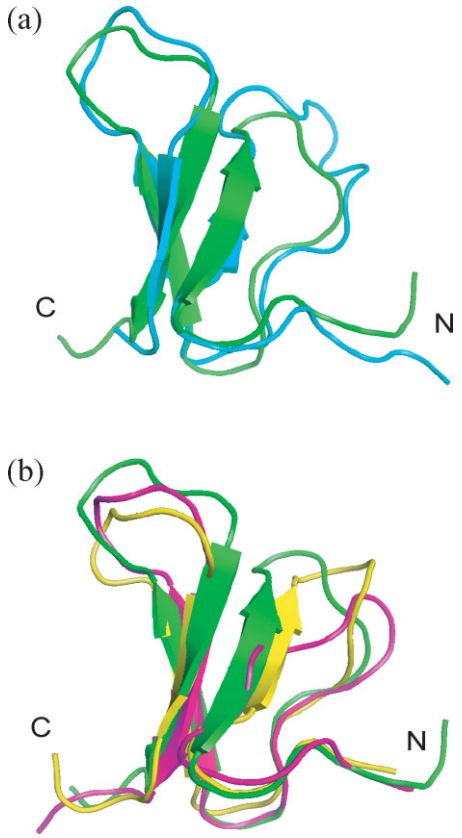

Figure 6 Structural comparisons of tachystatin B1 and other peptides with the ICK motif. (a) Overlay of the structures of tachystatin B1 (green) and tachystatin A2 (cyan; PDB ID: 1CIX) [20]. They could be fitted by the core ICK structures with the backbone atom RMSD of 1.00 Å. (b) Overlay of tachystatin B1 (green) on the structures of J-ATCX Hv1c (magenta; PDB ID: 1DL0) [46] and ATCX-Hi : OB4219 (yellow; PDB ID: 1KQH) [45]. They could be also fitted by the core ICK structures with the RMSD of 1.01 Å for tachystatin B1 and Janus-faced atracotoxin Hv1c and 1.05 Å for tachystatin B1 and atracotoxin-Hi : OB4219.

conformation [20]. However, the addition of charged residue Arg[17] in the long loop provided ambiguous amphiphilicity to tachystatin B, which could be one of the major causes of the loss of activity against *E. coli*.

The tachystatin family shows the sequence homology with neurotoxins isolated from funnel web spiders as shown in Figure 1 [21]. Particularly, the essential disulfide bonds for the ICK motif are strongly conserved between tachystatins and neurotoxins. In order to investigate the solution structure homology, as well as the primary structure, we have searched for other peptides with structural similarity to tachystatin B using the Dali server (http://www.ebi.ac.uk/dali/index.html [47]). Except for tachystatin A, 11 structures were hit with a Z-score greater than 2.0. For the structural comparison, two peptides with Z-scores greater than 4.0, Janus-faced atracotoxin Hv1c (J-ATCX Hv1c) and atracotoxin-Hi : OB4219 (ATCX-Hi : OB4219) isolated from the venom of Australian funnel web

DOI: 10.1002/psc

spiders *Hadronyche versuta* and *Hadronyche infensa sp*, respectively [45,46,] are superimposed with tachystatin B1 in Figure 6(b). When the backbone atoms of the core ICK structures of tachystatin B1 were fitted to those of J-ATCX Hv1c and ATCX-Hi:OB4219, the RMSDs of the superimposed region were found to be 1.01 Å and 1.05 Å, respectively. Their structures show great structural homology with deviation only in the long loop between β1 and β2. In spite of structural similarity with neurotoxic peptides, tachystatin B does not have neurotoxic activity. The ICK motif could be an ancestral protein folding and a versatile scaffold for molecular function. Neurotoxic peptides with the ICK motif might be developed from antimicrobial peptides in ancestral organism, and might acquire the additional function in molecular evolutionary processing.

Essential Residue for Chitin-binding

Tachystatin B has chitin-binding property as well as antimicrobial activity. Chitin-binding property would inseparably contribute to the antifungal activity because chitin is one of the major components of fungi cell wall. Recent studies on chitin-binding protein have reported that the essential residues for binding to chitin are the exposed aromatic residues [48–50]. In our previous study on tachystatin A, we also proposed two potential residues for binding to chitin [20]. One of them is Phe^{9} located on the first β-turn and another is Tyr^{16} in long loop between strands β1 and β2 [20]. There is Tyr^{14} in tachystatin B corresponding to Tyr^{16} of tachystatin A, although the aromatic residue corresponding to Phe^{9} of tachystatin A is missing. In the alignments of their primary structures (Figure 1), Tyr^{14} of tachystatin B and Tyr^{16} of tachystatin A are not located on the preserved position. However, both tyrosines are located on the same long loop between strands β1 and β2, and their positions on the three-dimensional structure are preserved (Figure 7). On the basis of the structure–function relationship, Tyr^{14} could be an essential residue for chitin-binding activity. Moreover, there should be the other residue for the chitin recognition because the chitin-binding activity of tachystatin B is stronger than that of tachystatin A [21]. The most different part between tachystatin B and tachystatin A is the long loop between strand β1 and β2. Tachystatin B contains positively charged Arg^{17} in the long loop, although there are no charged residues in the corresponding loop of tachystatin A. In the case of tachystatin B, this long loop may be an important structure for binding to chitin, as Tyr^{14} recognizes the nonpolar face of sugar ring by hydrophobic interaction, and the positively charged Arg^{17} binds to the polar face with electrostatic interaction.

CONCLUSIONS

The three-dimensional structures of tachystatin B have been determined by NMR experiments and structure calculations. Tachystatin B has a triple-stranded β-sheet and stabilized the ICK motif. The structural comparison with other ICK peptides led us to suggest that the ICK motif could be one of the most fundamental scaffolds for antimicrobial activity and the major active site might be located on the long loop between the first and second β-strands. Particularly, chitin-binding activity might be exerted by this long loop with the important residues Tyr^{14} and Arg^{17}. Along with cyclotides [51], the stability provided by the cystine-knot may be an essential structure for the development of antibiotic substances and may lead to design of mimetics.

Acknowledgements

This work was supported by a grant-in-aid for scientific research from Ministry of Education, Science, Sports,

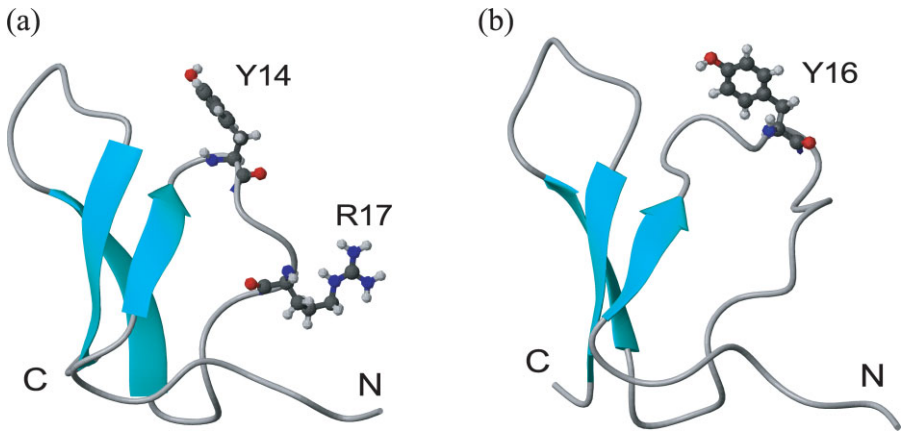

Figure 7 Essential residues for chitin-binding of tachystatin B and tachystatin A. (a) The ribbon model of tachystatin B1 with the essential residues (stick models) for chitin-binding property. (b) The ribbon model of tachystatin A2 (PDB ID: 1CIX) [20] with the essential residue (stick model) for the comparison with (a). The key residues for chitin binding are located on the long loop between strands β1 and β2.

DOI: 10.1002/psc

and Culture of Japan (17-8750 to N. F.) and the Program for the Promotion of Basic Research Activities for Innovative Biosciences, Japan.

REFERENCES

1. Hoffmann JA, Kafatos FC, Janeway CA Jr, Ezekowitz RAB. Phylogenetic perspectives in innate immunity. *Science* 1999; **284**: 1313–1318.
2. Salzet M. Vertebrate innate immunity resembles a mosaic of invertebrate immune responses. *Trends Immunol.* 2001; **22**: 285–288.
3. Hoebe K, Jansen E, Beutler B. The interface between innate and adaptive immunity. *Nat. Immunol.* 2004; **5**: 971–974.
4. Powers JP, Hancock RE. The relationship between peptide structure and antibacterial activity. *Peptides* 2003; **24**: 1681–1691.
5. Dimarcq JL, Bulet P, Hetru C, Hoffmann J. Cysteine-rich antimicrobial peptides in invertebrates. *Biopolymers* 1999; **47**: 465–477.
6. Zasloff M. Antimicrobial peptides of multicellular organisms. *Nature* 2002; **415**: 389–395.
7. Craik DJ, Daly NL, Waine C. The cystine knot motif in toxins and implications for drug design. *Toxicon* 2001; **39**: 43–60.
8. Iwanaga S, Kawabata S, Muta T. New types of clotting factors and defense molecules found in horseshoe crab hemolymph: their structures and functions. *J. Biochem. (Tokyo)* 1998; **123**: 1–15.
9. Iwanaga S. The molecular basis of innate immunity in the horseshoe crab. *Curr. Opin. Immunol.* 2002; **14**: 87–95.
10. Iwanaga S, Lee BL. Recent advances in the innate immunity of invertebrate animals. *J. Biochem. Mol. Biol.* 2005; **38**: 128–150.
11. Toh Y, Mizutani A, Tokunaga F, Muta T, Iwanaga S. Morphology of the granular hemocytes of the Japanese horseshoe crab *Tachypleus tridentatus* and immunocytochemical localization of clotting factors and antimicrobial substances. *Cell Tissue Res.* 1991; **266**: 137–147.
12. Kawabata S, Muta T, Iwanaga S. Clotting cascade and defense molecules found in the hemolymph of the horseshoe crab. In *New Directions in Invertebrate Immunology*, Söderhäll K, Iwanaga S, Vasta GR (eds). SOS Publications: Fair Haven, NJ, 1996; 255–283.
13. Muta T, Iwanaga S. The role of hemolymph coagulation in innate immunity. *Curr. Opin. Immunol.* 1996; **8**: 41–47.
14. Beisel HG, Kawabata S, Iwanaga S, Huber R, Bode W. Tachylectin-2: crystal structure of a specific GlcNAc/GalNAc-binding lectin involved in the innate immunity host defense of the Japanese horseshoe crab *Tachypleus tridentatus*. *EMBO J.* 1999; **18**: 2313–2322.
15. Kairies N, Beisel HG, Fuentes-Prior P, Tsuda R, Muta T, Iwanaga S, Bode W, Huber R, Kawabata S. The 2.0-Å crystal structure of tachylectin 5A provides evidence for the common origin of the innate immunity and the blood coagulation systems. *Proc. Natl. Acad. Sci. U.S.A.* 2001; **98**: 13519–13524.
16. Bergner A, Oganessyan V, Muta T, Iwanaga S, Typke D, Huber R, Bode W. Crystal structure of limulus coagulogen: the clotting protein from horseshoe crab, a structural homologue of nerve growth factor. *EMBO J.* 1996; **15**: 6789–6797.
17. Kawano K, Yoneya T, Miyata T, Yoshikawa K, Tokunaga F, Terada Y, Iwanaga S. Antimicrobial peptide, tachyplesin I, isolated from hemocytes of the horseshoe crab (*Tachypleus tridentatus*). *J. Biol. Chem.* 1990; **265**: 15365–15367.
18. Laederach A, Andreotti AH, Fulton DB. Solution and micelle-bound structures of tachyplesin I and its active aromatic linear derivatives. *Biochemistry* 2002; **41**: 12359–12368.
19. Suetake T, Tsuda S, Kawabata S, Miura K, Iwanaga S, Hikichi K, Nitta K, Kawano K. Chitin-binding proteins in invertebrates and plants comprise a common chitin-binding structural motif. *J. Biol. Chem.* 2000; **275**: 17929–17932.
20. Fujitani N, Kawabata S, Osaki T, Kumaki Y, Demura M, Nitta T, Kawano K. Structure of the antimicrobial peptide tachystatin A. *J. Biol. Chem.* 2002; **277**: 23651–23657.
21. Osaki T, Omotezako M, Nagayama R, Hirata M, Iwanaga S, Kasahara J, Hattori J, Ito I, Sugiyama H, Kawabata S. Horseshoe crab hemocyte-derived antimicrobial polypeptides, tachystatins, with sequence similarity to spider neurotoxins. *J. Biol. Chem.* 1999; **274**: 26172–26178.
22. Nakamura T, Furunaka H, Miyata T, Tokunaga F, Muta T, Iwanaga S, Niwa M, Takao T, Shimonishi Y. Tachyplesin, a class of antimicrobial peptide from the hemocytes of the horseshoe crab (*Tachypleus tridentatus*). *J. Biol. Chem.* 1988; **263**: 16709–16713.
23. Rance M, Sørensen OW, Bodenhausen G, Wagner G, Ernst RR, Wüthrich K. Improved spectral resolution in COSY ^{1}H NMR spectra of proteins via double quantum filtering. *Biochem. Biophys. Res. Commun.* 1983; **117**: 479–485.
24. Braunschweiler L, Ernst RR. Coherence transfer by isotropic mixing: application to proton correlation spectroscopy. *J. Magn. Reson.* 1983; **53**: 521–528.
25. Bax A, Davis DG. MLEV-17-based two-dimensional homonuclear magnetization transfer spectroscopy. *J. Magn. Reson.* 1985; **65**: 355–360.
26. Jeener J, Meier BN, Bachmann P, Ernst RR. Investigation of exchange processes by two-dimensional NMR spectroscopy. *J. Chem. Phys.* 1979; **71**: 4546–4553.
27. Piotto M, Saudek V, Sklenár V. Gradient-tailored excitation for single-quantum NMR spectroscopy of aqueous solutions. *J. Biomol. NMR* 1992; **2**: 661–665.
28. Sklenár V, Piotto M, Leppik R, Saudek V. Gradient-tailored water suppression for ^{1}H–^{15}N HSQC experiments optimized to retain full sensitivity. *J. Magn. Reson., Ser. A* 1993; **102**: 241–245.
29. Delaglio F, Grzesiek S, Vuister G, Zhu G, Pfeifer J, Bax A. NMRPipe: a multidimensional spectral processing system based on UNIX pipes. *J. Biomol. NMR* 1995; **6**: 277–293.
30. Bartels C, Xia TH, Billeter M, Güntert P, Wüthrich K. The program XEASY for computer-supported NMR spectral analysis of biological macromolecules. *J. Biomol. NMR* 1995; **6**: 1–10.
31. Wüthrich K. *NMR of Proteins and Nucleic Acids*. John Wiley and Sons: New York, 1986.
32. Griesinger C, Sørensen OW, Ernst RR. Two-dimensional correlation of connected NMR transitions. *J. Am. Chem. Soc.* 1985; **107**: 6394–6396.
33. Jones JA, Wilkins DK, Smith LJ, Dobson CM. Characterization of protein unfolding by NMR diffusion measurements. *J. Biomol. NMR* 1997; **10**: 199–203.
34. Wilkins DK, Grimshaw SB, Receveur V, Dobson CM, Jones JA, Smith LJ. Hydrodynamic radii of native and denatured proteins measured by pulse field gradient NMR techniques. *Biochemistry* 1999; **38**: 16424–16431.
35. Wu DH, Chen AD, Johnson CS Jr. An improved diffusion-ordered spectroscopy experiment incorporating bipolar-gradient pulses. *J. Magn. Reson.* 1995; **115**: 260–264.
36. Brünger AT, Adams PD, Clore GM, DeLano WL, Gros P, Grosse-Kunstleve RW, Jiang JS, Kuszewski J, Nilges M, Pannu NS, Read RJ, Rice LM, Simonson T, Warren GL. Crystallography & NMR system: a new software suite for macromolecular structure determination. *Acta Crystallogr., Sect. D* 1998; **54**: 905–921.
37. Schibli DJ, Hunter HN, Aseyev V, Starner TD, Wiencek JM, McCray PB Jr, Tack BF, Vogel HJ. The solution structures of the human β-defensins lead to a better understanding of the potent bactericidal activity of HBD3 against *Staphylococcus aureus*. *J. Biol. Chem.* 2002; **277**: 8279–8289.
38. Laskowski RA, Rullmann JAC, MacArthur MW, Kaptein R, Thornton JM. AQUA and PROCHECK-NMR: programs for checking the quality of protein structures solved by NMR. *J. Biomol. NMR* 1996; **8**: 477–486.
39. Koradi R, Billeter M, Wüthrich K. MOLMOL: a program for display and analysis of macromolecular structures. *J. Mol. Graphics* 1996; **14**: 51–55.

40. Pallaghy PK, Nielsen KJ, Craik DJ, Norton RS. A common structural motif incorporating a cystine knot and a triple-stranded β-sheet in toxic and inhibitory polypeptides. *Protein Sci.* 1994; **3**: 1833–1839.
41. Norton RS, Pallaghy PK. The cystine knot structure of ion chabbel toxins and related polypeptides. *Toxicon* 1998; **36**: 1573–1583.
42. Skoog B, Wichman A. Calculation of the isoelectric points of polypeptides from the amino acid composition. *Trends Anal. Chem.* 1986; **5**: 82–83.
43. Fletcher JI, Smith R, O'Donoghue SI, Nilges M, Connor M, Howden ME, Christie MJ, King GF. The structure of a novel insecticidal neurotoxin, ω-agatoxin-HV_1, from the venom of an Australian funnel web spider. *Nat. Struct. Biol.* 1997; **4**: 559–566.
44. Hancock RE, Falla T, Brown M. Cationic bactericidal peptides. *Adv. Microb. Physiol.* 1995; **37**: 135–175.
45. Rosengren KJ, Wilson D, Daly NL, Alewood PF, Craik DJ. Solution structures of the *cis*- and *trans*-Pro30 isomers of a novel 38-residue toxin from the venom of *Hadronyche infensa sp.* that contains a cystine-knot motif within its four disulfide bonds. *Biochemistry* 2002; **41**: 3294–3301.
46. Wang XH, Connor M, Smith R, Maciejewski MW, Howden MEH, Nicholson GM, Christie MJ, King GF. Discovery and characterization of a family of insecticidal neurotoxins with a rare vicinal disulfide bridge. *Nat. Struct. Biol.* 2000; **7**: 505–513.
47. Holm L, Sander C. Mapping the protein universe. *Science* 1996; **273**: 595–602.
48. Vaaje-Kolstad G, Houston DR, Riemen AH, Eijsink VG, van Aalten DM. Crystal structure and binding properties of the Serratia marcescens chitin-binding protein CBP21. *J. Biol. Chem.* 2005; **280**: 11313–11319.
49. Xiang Y, Huang RH, Liu XZ, Zhang Y, Wang DC. Crystal structure of a novel antifungal protein distinct with five disulfide bridges from *Eucommia ulmoides* Oliver at an atomic resolution. *J. Struct. Biol.* 2004; **148**: 86–97.
50. Huang RH, Xiang Y, Tu GZ, Zhang Y, Wang DC. Solution structure of *Eucommia* antifungal peptide: a novel structural model distinct with a five-disulfide motif. *Biochemistry* 2004; **43**: 6005–6012.
51. Tam JP, Lu YA, Yang JL, Chiu KW. An unusual structural motif of antimicrobial peptides containing end-to-end macrocycle and cysteine-knot disulfides. *Proc. Natl. Acad. Sci. U.S.A.* 1999; **96**: 8913–8918.

DOI: 10.1002/psc